Hypoxia of the growing liver accelerates regeneration

Schadde, Erik ; Tsatsaris, Christopher ; Swiderska-Syn, Marzena ; Breitenstein, Stefan ; Urner, Martin ; Schimmer, Roman ; Booy, Christa ; Z'graggen, Birgit Roth ; Wenger, Roland H ; Spahn, Donat R ; Hertl, Martin ; Knechtle, Stuart ; Diehl, Ann Mae ; Schläpfer, Martin ; Beck-Schimmer, Beatrice

Abstract: Background. After portal vein ligation of 1 side of the liver, the other side regenerates at a slow rate. This slow growth may be accelerated to rapid growth by adding a transection between the 2 sides, i.e., performing portal vein ligation and parenchymal transection. We found that in patients undergoing portal vein ligation and parenchymal transection, portal vein hyperflow in the regenerating liver causes a significant reduction of arterial flow due to the hepatic arterial buffer response. We postulated that the reduction of arterial flow induces hypoxia in the regenerating liver and used a rat model to assess hypoxia and its impact on kinetic growth. Methods. A rat model of rapid (portal vein ligation and parenchymal transection) and slow regeneration (portal vein ligation) was established. Portal vein flow and pressure data were collected. Liver regeneration was assessed in rats using computed tomography, proliferation with Ki-67, and hypoxia with pimonidazole and HIF-1a staining. Results. The rat model confirmed acceleration of regeneration in portal vein ligation and parenchymal transection as well as the portal vein hyperflow seen in patients. Additionally, tissue hypoxia was observed after portal vein ligation and parenchymal transection, while little hypoxia staining was detected after portal vein ligation. To determine if hypoxia is a consequence or an inciting stimulus of rapid liver regeneration, we used a prolyl-hydroxylase blocker to activate hypoxia signaling pathways in the slow model. This clearly accelerated slow to rapid liver regeneration. Inversely, abrogation of hypoxia led to a blunting of rapid growth to slow growth. The topical application of prolyl-hydroxylase inhibitors on livers in rats induced spontaneous areas of regeneration. Conclusion. This study shows that pharmacologically induced hypoxic signaling accelerates liver regeneration similar to portal vein ligation and parenchymal transection. Hypoxia is likely an accelerator of liver regeneration. Also, prolyl-hydroxylase inhibitors may be used to enhance liver regeneration pharmaceutically.

DOI: https://doi.org/10.1016/j.surg.2016.05.018

Schadde, Erik; Tsatsaris, Christopher; Swiderska-Syn, Marzena; Breitenstein, Stefan; Urner, Martin; Schimmer, Roman; Booy, Christa; Z'graggen, Birgit Roth; Wenger, Roland H; Spahn, Donat R; Hertl, Martin; Knechtle, Stuart; Diehl, Ann Mae; Schläpfer, Martin; Beck-Schimmer, Beatrice (2017). Hypoxia of the growing liver accelerates regeneration. Surgery, 161(3):666-679.
DOI: https://doi.org/10.1016/j.surg.2016.05.018

Hypoxia of the growing liver accelerates regeneration

Erik Schadde, MD,[a,b,c] Christopher Tsatsaris, MD,[a] Marzena Swiderska-Syn, DVM,[d] Stefan Breitenstein, MD,[c] Martin Urner, MD,[a,e] Roman Schimmer, BSc,[a] Christa Booy,[a] Birgit Roth Z'graggen, PhD,[a] Roland H. Wenger, PhD,[a] Donat R. Spahn, MD,[e] Martin Hertl, MD, PhD,[b] Stuart Knechtle, MD,[f] Ann Mae Diehl, MD, PhD,[d] Martin Schläpfer, MD, MSc,[a,e,*] *and* **Beatrice Beck-Schimmer, MD,[a,e,g,*]** *Zürich, Switzerland, Chicago, IL, and Durham, NC*

Background. *After portal vein ligation of 1 side of the liver, the other side regenerates at a slow rate. This slow growth may be accelerated to rapid growth by adding a transection between the 2 sides, i.e., performing portal vein ligation and parenchymal transection. We found that in patients undergoing portal vein ligation and parenchymal transection, portal vein hyperflow in the regenerating liver causes a significant reduction of arterial flow due to the hepatic arterial buffer response. We postulated that the reduction of arterial flow induces hypoxia in the regenerating liver and used a rat model to assess hypoxia and its impact on kinetic growth.*

Methods. *A rat model of rapid (portal vein ligation and parenchymal transection) and slow regeneration (portal vein ligation) was established. Portal vein flow and pressure data were collected. Liver regeneration was assessed in rats using computed tomography, proliferation with Ki-67, and hypoxia with pimonidazole and HIF-1α staining.*

Results. *The rat model confirmed acceleration of regeneration in portal vein ligation and parenchymal transection as well as the portal vein hyperflow seen in patients. Additionally, tissue hypoxia was observed after portal vein ligation and parenchymal transection, while little hypoxia staining was detected after portal vein ligation. To determine if hypoxia is a consequence or an inciting stimulus of rapid liver regeneration, we used a prolyl-hydroxylase blocker to activate hypoxia signaling pathways in the slow model. This clearly accelerated slow to rapid liver regeneration. Inversely, abrogation of hypoxia led to a blunting of rapid growth to slow growth. The topical application of prolyl-hydroxylase inhibitors on livers in rats induced spontaneous areas of regeneration.*

Conclusion. *This study shows that pharmacologically induced hypoxic signaling accelerates liver regeneration similar to portal vein ligation and parenchymal transection. Hypoxia is likely an accelerator of liver regeneration. Also, prolyl-hydroxylase inhibitors may be used to enhance liver regeneration pharmaceutically. (Surgery 2016;■:■-■.)*

From the Institute of Physiology,[a] Center for Integrative Human Physiology, University of Zürich, Zürich, Switzerland; Division of Transplant Surgery, Department of Surgery,[b] Rush University Medical Center, Chicago, IL; Department of Surgery, Cantonal Hospital Winterthur,[c] Zürich, Switzerland; Division of Hepatology, Department of Gastroenterology[d] and Division of Transplantation, Department of Surgery,[f] Duke University, Durham, NC; Institute of Anesthesiology,[e] University Hospital Zürich, Zürich, Switzerland; Department of Anesthesiology,[g] University of Illinois Chicago, Chicago, IL

The liver regenerates extensively after injury to hepatocytes, partial removal of liver tissue (partial hepatectomy), and upon flow abrogation of 1 of the 2 portal vein branches.[1] Portal vein occlusion may be achieved either through interventional embolization or surgical ligation, while the hepatic artery supplies oxygen and nutrition to the ligated lobe. This maneuver, first described by liver surgeons almost 30 years ago,[2] results in growth of the nonligated part of the liver. Liver regeneration after portal vein manipulation found its clinical application in liver operations performed to increase the size of the disease-free liver prior to extensive resections.[3] With this application, removal of previously unresectable liver tumors with extended hepatectomies became possible.

*Authors contributed equally as last authors.

Accepted for publication May 17, 2016.

Reprint requests: Erik Schadde, MD, Institute of Physiology, University of Zürich, Winterthurerstr. 190, CH-8057 Zürich, Switzerland. E-mail: erik.schadde@uzh.ch.

0039-6060/$ - see front matter

http://dx.doi.org/10.1016/j.surg.2016.05.018

Portal vein occlusion results in only a moderate amount of hypertrophy: 30–40% in 4–6 weeks.[3] In contrast, >50% hepatectomy is associated with a rapid and extensive regeneration with the degree of hypertrophy at 80–90% within 10 days.[4] It is interesting to note that, in contrast to partial hepatectomy, no tissue is removed during portal vein occlusion. The observation that the liver regenerates after redirection of portal flow alone has led to the hypothesis that changes in portal vein hemodynamics may be contributing signals for liver regeneration.[5]

This hypothesis has raised renewed interest after a recent discovery: transection between the right and left lobes in addition to portal vein ligation (PVL + T) in humans, without any liver mass removal, accelerates slow regeneration induced by portal vein ligation (PVL) alone.[6] This manipulation induces extreme and rapid regeneration prior to resection and allows for extended liver resections after a week of waiting. The novel procedure in patients has been called "in-situ split hepatectomy" or "ALPPS" (Associating Liver Partition and Portal vein ligation for Staged hepatectomy), and it induces the same kinetic growth rate as partial hepatectomy (ie, rapid regeneration).[7] The observation has attracted considerable interest from liver surgeons because it allows in-situ liver regeneration of an unknown extent.[8] Also, adding simple tourniquet ligation of the parenchyma to contralateral PVL has been found to achieve the same kinetic growth rate as a more aggressive surgical procedure with transection between the lobes.[9]

Due to the obliteration of collaterals and intrahepatic shunts by the added transection, a possible trigger for rapid regeneration in the PVL + T model may be the hyperflow in the portal vein (ie, more volume flow per volume unit of liver tissue), while experimental evidence is missing.[10,11] In the presence of portal hyperflow, there has been longstanding evidence of a "buffer response" of the hepatic artery.[11] Upon increase of portal vein flow per volume of tissue, the hepatic artery flow decreases accordingly to allow constant total sinusoidal blood flow. Since the oxygenation of liver tissue depends largely on the hepatic artery, we hypothesized that PVL + T leads to hypoxia, which in turn may be a stimulus of accelerated regeneration in the growing liver. We used a rat model of PVL and PVL + T to test this hypothesis.

METHODS

Human studies. Approval to perform the surgical procedure of PVL + T, the first stage of ALPPS, in patients was obtained from the Ethics Committee of the Kanton of Zurich in the context of a prospective international registry (NCT01924741). Consents for collection of intra- and perioperative data were obtained from patients.

Portal vein ligation plus transection in human patients. PVL + T was performed at 2 hospitals (University Hospital Zurich and Kantonsspital Winterthur, Switzerland), as previously described.[12]

Hemodynamic measurements in human patients. Portal vein flow was measured using 16-mm flow probes (Transonic, Ithaca, NY), and hepatic artery flow was measured using 4-mm flow probes, expressed in mL/min. Portal vein pressure was measured using Draeger Infinity Monitoring system (Draeger, Lübeck, Germany).

Animals. Approval for the experiments was obtained from the Veterinary Authorities of the Canton of Zurich, Switzerland (number 60/2014). All experiments with male Wistar rats (Charles River, Sulzfeld, Germany) were performed in compliance with the guidelines for Experiments on Animals by the Swiss Academy of Medical Sciences and the Federation of European Laboratory Animal Science Associations guidelines. To help condition them for the procedure, rats were kept in ventilated cages (4 rats each) under standard pathogen-free conditions in a 12/12-hour light/dark cycle for at least 5 days prior to the performance of the procedure. The ambient temperature was 22 ± 1°C. Food and water were provided ad libitum. The median weight of the animals was 265 g (interquartile range [IQR] 250–295). We performed the volumetric studies by computed tomographic (CT) imaging in 5 rats per group. Likewise for tissue and blood samples, groups of 5 animals were killed at each time point. The exact number of animals per experiment (n) is indicated in the figures.

Anesthesia animals. During all operative procedures, animals were allowed to breathe spontaneously under isoflurane anesthesia (Attane, Piramal, Mumbai, India), 1.0–2.5 vol% vaporized in 600 mL oxygen/min. Analgesia was provided using a standard protocol of subcutaneous buprenorphine injections.

Model of slow and rapid liver regeneration after PVL in rats. To develop models of slow and rapid liver regeneration in rats, the right middle lobe (RML 25% of total liver volume) Fig 1, *A* was chosen as the liver remnant. Slow liver regeneration (PVL, Fig 1, *A*) of the RML was induced by ligating the portal vein of the right, the caudate, and the left lateral lobe using 6-0 silk ties (Fig 1). Rapid regeneration (PVL+T, Fig 1, *A*) was induced by

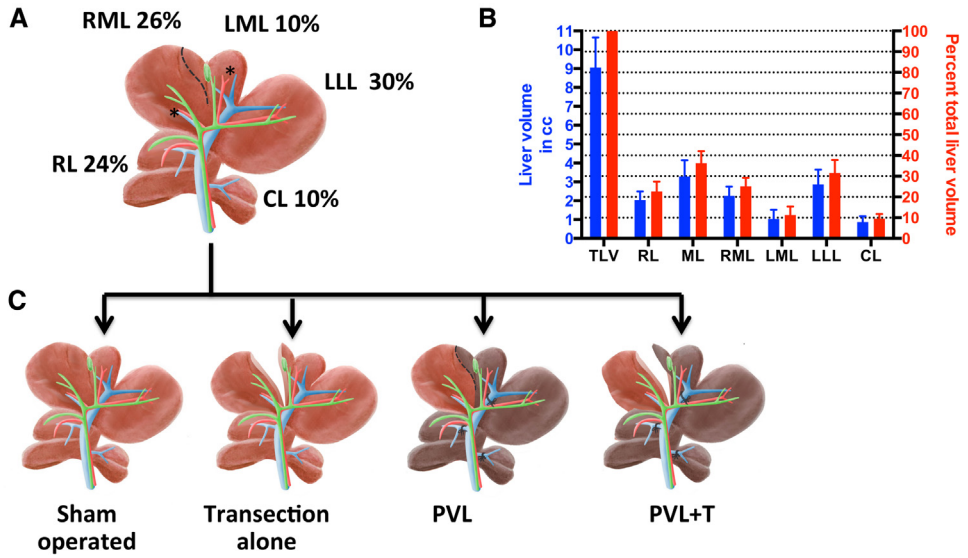

Fig 1. Anatomy and baseline volumetry of the rat liver and portal vein ligation models. (*A*) Anatomy of the 4 lobes of the rat liver: right lobe (RL); middle lobe (ML) with right (RML) and left middle lobe (LML); left lateral lobe (LLL); caudate lobe (CL). The ML is the only lobe supplied by 2 separate portal vein branches (*), taking off directly from the main portal vein and is therefore the only lobe suitable for transection in the rat liver. (*B*) Absolute and relative volumes of liver lobes as assessed in 16 Wistar rats undergoing computerized tomographic volumetry with intravenously applied contrast. The largest lobe is the ML (36%), which may be divided into RML (26%) and LML (10%). (*C*) Models of regeneration compared in this study. The surgical transection line divides the ML into the right middle lobe (RML) and the left middle lobe (LML). In portal vein ligation (PVL), the portal veins supplying the right, left lateral, left middle, and caudate lobe are ligated using silk ligatures. When the portal vein is ligated and the ML transected between RML and LML, the model is called portal vein ligation and transection (PVL + T). In animals with transection alone, the ML is transected, but the portal vein blood supply to both lobes remains normal. In sham-operated animals, nonoccluding ties are placed around the portal veins.

additionally transecting along the ischemic line with a nonsticking bipolar microforceps (Supergliss, Sutter GmbH, Freiburg i.B., Germany; PVL + T). Sham operations with loose, nonoccluding ligatures around the respective portal veins (sham operated, Fig 1, *C*), and only transection between RML and left middle lobe (transection alone, Fig 2, *C*) were used as controls.

Application of dimethyloxalylglycine. Twelve hours before the operation dimethyloxalylglycine ([DMOG] Axxora Ltd, Nottingham, UK) was intraperitoneally administered (200 μg/g body weight).[13] To examine the incidentally discovered topical effect of DMOG on liver proliferation, we used a small paint brush to apply the DMOG solution onto livers.

Application of myo-inositol-trispyrophosphate. Myo-inositol-trispyrophosphate ([ITPP] Carbosynth, Compton, Berkshire, UK) was dissolved in normal saline (200 mg/mL) and administered by intraperitoneal injection of 0.3 mg/g of body weight each, 12 hours before the operation.[14] On the first postoperative day, 0.1 mg/g of body weight was again applied.

Hemodynamic measurements in rats. To assess portal flow, 2-mm flow probes (Transonic, Ithaca, NY) were used. Volume flow probes measure volume directly rather than extrapolating from flow velocity and vessel diameter. Portal vein pressure was determined using pressure transducers and anesthesia monitors (Dräger, Lübeck, Germany).

Volumetry of rat livers. To assess regeneration of the RML, animals underwent repetitive CT and volumetry scanning every 24 hours for up to 72 hours (Quantum FX MicroCT, PerkinElmer, Waltham, MA) after prior intravenous injection of 200 μL of the contrast ExiTron nano 12,000 (Miltenyi Biotech, Bergisch Gladbach, Germany).

Pimonidazole staining to quantify tissue oxygenation. Pimonidazole was dissolved in normal saline (100 mg/mL), and 60 mg were injected intravenously 1 hour prior to harvesting the organs.[15] Pimonidazole undergoes chemical reduction under hypoxic conditions, binds irreversibly to SH-containing molecules, such as glutathione and proteins, and the resulting complexes accumulate in hypoxic tissue. The pimonidazole bound

in tissue was visualized with monoclonal antibodies using immunofluorescence.

Histochemistry and immunofluorescence. Cryosections of 6 μm were fixed using acetone (Sigma Aldrich, St. Louis, MO) for pimonidazole staining or paraformaldehyde 4% (Sigma Aldrich) for 10 minutes at room temperature for Ki-67 staining. After 10 minutes, slides were kept in ice-cold phosphate-buffered saline (PBS, Kantonsapotheke Zurich, Switzerland) before the individual protocols were started. Slides were washed 3 times for 5 minutes; then, they were blocked at room temperature for at least 1 hour using 10% goat serum (Sigma-Aldrich) with 1% bovine serum albumin for pimonidazole staining or with 1 × PBS+5% goat serum + 0.3% Triton X-100 for Ki-67 staining. Incubation with the primary antibody took place at 4°C overnight. The following day a staining with an appropriate fluorochrome-coupled secondary antibody took place for 2 hours at room temperature; nuclei were stained using 4,6-diamidin-2-phenylindol (DAPI, Roche, Rotkreuz, Zug, Switzerland).

For staining of hypoxia-inducible factor-1α (HIF-1α), formalin-fixed, paraffin-embedded liver tissue was cut into 5 μm sections and placed on glass slides. Sections were deparaffinized with xylene, dehydrated with ethanol, and then incubated with 3% hydrogen peroxide to block endogenous peroxidase. Antigen retrieval was performed by heating in 10 mM sodium citrate buffer (pH 6.0). Sections were blocked in DAKO protein block (X9090; DAKO, Glostrup, Denmark), followed by incubation with primary antibodies, rabbit anti-HIF-1α (Abcam 2185, diluted 1:800; Cambridge, UK); secondary antibodies were used to visualize target proteins. DAB reagent (K3466; DAKO) was applied in the detection procedure. Tissue sections were counterstained with Aqua Hematoxylin-INNOVEX (Innovex Biosciences, Richmond, CA). Negative controls included liver specimens exposed to 1% bovine serum albumin instead of to the respective primary antibodies. The number of detected HIF-1α immunoreactive cells was quantified by counting in 20–40 randomly chosen, 20× fields per section per animal.

The following primary antibodies were used: rabbit anti-Ki-67 (Abcam, diluted 1:400) and rabbit anti-pimonidazole (Hypoxyprobe, MA; diluted 1:200). Slides were mounted with ProLong Gold Antifade Mountant (Life Technologies, Zug, Switzerland).

Image acquisition and processing. Immunofluorescence images were acquired with the Slidescanner Axio Scan.Z1 (Zeiss, Feldbach, Zurich, Switzerland) and the ZEN blue (Zeiss) image-processing and analyzing software. A 20× objective with aperture was used; the maximal intensity was set to 5,247.

Determination of mean fluorescence intensity in pimonidazole-stained liver slices. Image analysis was performed using R: a language and environment for statistical computing[16] and the EBImage, an R package for imaging processing with applications to cellular phenotypes (R Foundation for Statistical Computing, Vienna, Austria).[17] Briefly, variance in fluorescence intensity of liver slices was expressed in relation to positive control (hepatic artery ligation, mean variance = 100%) and negative control (sham surgery, mean variance = 0%). The R code of this procedure is included in the online only Data supplement.

Generation of a fusion image based on DAPI- and Ki-67-stained liver slices and quantification of Ki-67-positive cells. Red, green, blue (RGB) fusion images from DAPI- and Ki-67–stained liver slices were computed using R[16] and the EBImage package.[17] Matching DAPI- and Ki-67-stained fluorescence spots were also highlighted as red spots using the "paintObjects" function. The R code of this procedure is enclosed in the online only Data supplement. The number of Ki-67 positive cells was determined by evaluation of 5 random visual fields at 200× magnification.

Experimental outcomes and statistical methods. The primary outcome was liver hypertrophy measured volumetrically in 24-hour intervals after PVL and PVL + T. Secondary outcomes were proliferation as assessed by KI-67 staining. Data are means and standard deviations (SDs) for normally distributed data, median, and IQR for skewed data. For comparisons of normally distributed groups, we used the Student *t* test (2 groups) or analysis of variance ([ANOVA] for >2 groups) with Sidak-correction for multiple comparisons. Details on the statistical analysis used for each experiment are given in legends to Figs 2-6. Prism 6.0 (GraphPad Software Inc, San Diego, CA) was used for data analysis and presentation.

RESULTS

Right middle lobe serves as the regenerating lobe in the rat model. The rat liver consists of right, middle, left lateral, and caudate lobes (Fig 1, *A*). Small animal CT with intravenously applied contrast injection allowed assessment of the volumes of each lobe in an exact manner (Fig 1, *B*). The only lobe in rodents that has inflow from 2 separate portal veins and may serve as a model

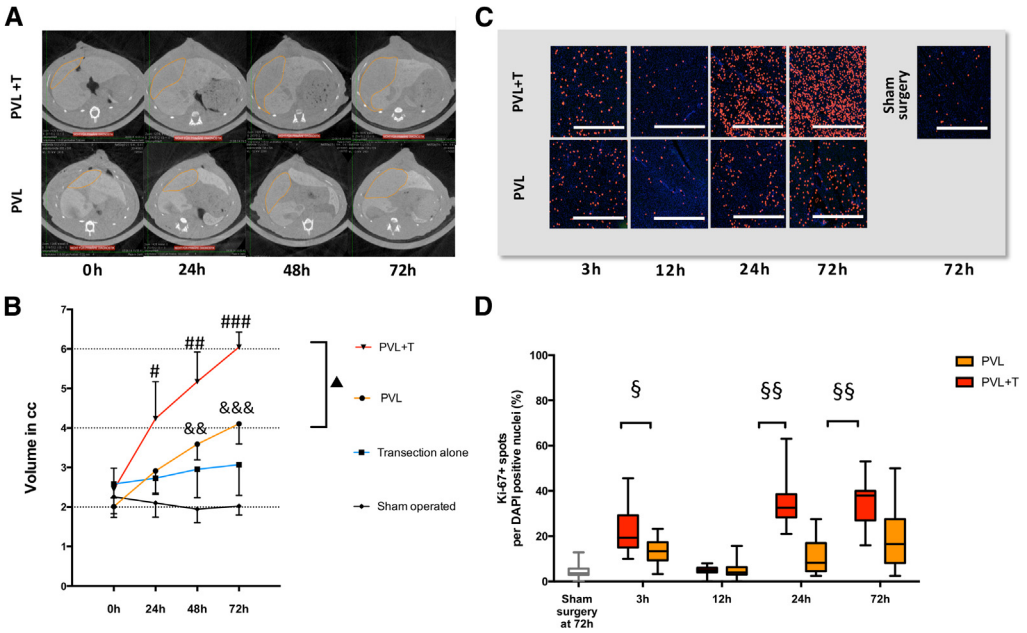

Fig 2. Evaluation of growth kinetics in models of portal vein ligation using computerized tomographic (CT) volumetry and immunofluorescence with Ki-67. (*A*) Small animal CT allows for an exact assessment of the volume of the regenerating right middle lobe (RML): the orange line at 24, 48, and 72 hours after intravenous injection of a nanoparticle-based contrast material. The regenerating RML appears less radio-opaque as it increases in size and is clearly delineated. Representative scans for both portal vein ligation (PVL) and portal vein ligation and transection (PVL + T) are shown. (*B*) Growth curves with means and standard deviations of liver volumes assessed by CT. Volume of the RML increases significantly compared with sham-operated animals at 24 hours in animals undergoing PVL + T ($n = 5$, $\#P = .01$); at 48 hours in animals undergoing PVL ($n = 5$, $\&\&P = .001$) and PVL + T ($\#\#P < .001$); at 72 hours in animals undergoing PVL ($\&\&\&P = .006$) and PVL + T ($\#\#\#P < .001$). Transection alone does not lead to a significant volume increase in the RML or other liver lobes ($n = 5$). Differences at 72 hours between PVL and PVL + T are significant ($\blacktriangle P = .001$), ANOVA was used for comparison of groups. (*C*) Differential regeneration is histologically evaluated using immunofluorescence with anti-Ki-67 antibody, marking mitotically active cells (*red*) in a background of nuclear staining (DAPI, *blue*) at 3, 12, 24, and 72 hours after PVL and after PVL + T at 72 hours (white scale bar = 1,000 μm). (*D*) Box plots with means and ranges of the proportion of Ki-67-positive nuclei per DAPI-stained cell nuclei as counted in 20 high-power fields. PVL and PVL + T are compared using ANOVA and multiple comparisons. A significantly higher percentage of Ki-67 positive cells is observed in PVL + T compared with PVL at 3 hours ($\S P = .009$), 24 hours ($\S\S P < .001$), and 72 hours ($\S\S P < .001$; $n = 5$ for each group), but not at 12 hours.

for selective portal vein ligation, with or without transection, is the middle lobe. We used the RML as the regenerating lobe, because the portal vein to the RML can be ligated easily, while ligation of the portal vein to the LML requires resection of the left lateral lobe and thereby a mass reduction of the liver, which we tried to avoid. The RML had a volume of 2.4 ± 0.5 mL or 26% of the total liver in rats with a median weight of 265 g. In humans, a remnant volume of <30% generally requires a procedure to increase the remnant volume before resection.[3] Figure 1, *C* shows the types of portal vein occlusion procedures performed to induce slow regeneration with PVL and rapid regeneration with PVL + T.

Transection between lobes accelerates regeneration in the rat model. Representative CT scans performed every 24 hours to assess the volume increase of the RML are shown in Fig 2, *A*. Fine lines drawn around the regenerating lobe to measure volume without sacrificing the animals are highlighted (Fig 2, *A*). PVL and PVL + T resulted in a significant volume increase within 24 hours after the operation of 44% and 74%, respectively, while the sham-operated group showed no change in liver volume (Fig 2, *B*). After 72 hours of continuous growth, the relative volume increase of PVL and PVL + T was 104% and 147% of the starting volume, respectively; sham-operated animals did not show significant changes in liver volume. PVL + T led to a significantly higher volume increase when compared with ligation alone.

The fraction of Ki-67 positive cells was evaluated using immunofluorescence with evaluation of

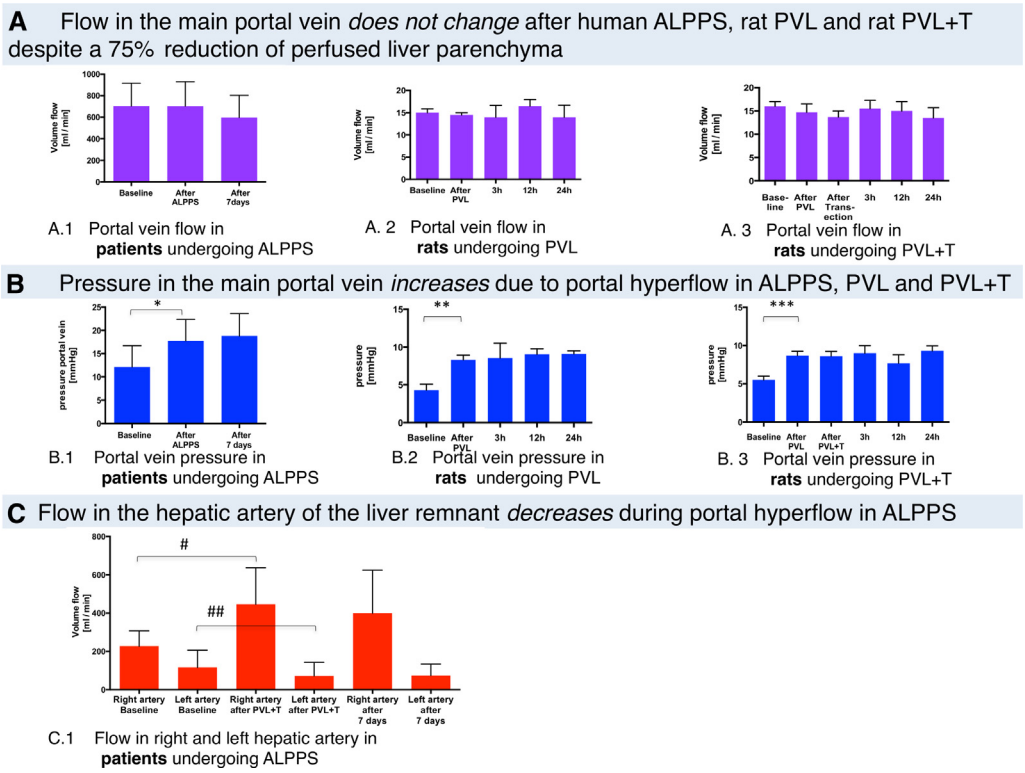

Fig 3. Flow and pressure studies of the human and rat main portal vein. (*A*) Volume flow in the main portal vein remains unchanged despite a 75% portal vein ligation (PVL) and PVL with transection (PVL + T), resulting in portal hyperflow. (*A1*) In patients, main portal vein volume flow is 705 ± 219 mL/min and remains unchanged immediately after right PVL + T and after re-exploration 7 days later ($P = .292$, $n = 15$). (*A2*) In rats, main portal volume flow does not change from a baseline of 15 mL/min (IQR 12–16) after PVL ($P = .198$, $n = 12$). (*A3*) In rats, there is also no difference in portal flow after PVL + T ($P = .281$, $n = 17$) for up to 24 hours. (*B*) Portal hyperflow results in increase in portal vein pressure. (*B1*) In patients, main portal vein pressure increases from 12 ± 5 to 18 ± 4 mm Hg after PVL + T (*$P = .002$), and the pressure stays elevated for up to 7 days at re-exploration ($n = 15$). (*B2*) In rats, portal vein pressure increases from 4.3 (IQR 3.7–5.1) to 8.3 (IQR 7.0–8.6) mm Hg after PVL (**$P = .004$, $n = 12$). (*B3*) In rats, pressure increases during the PVL step from 5.5 (IQR 4.7–6.0) to 8.7 (IQR 7.6–9.3) mm Hg (***$P = .001$, $n = 17$) and does not change thereafter. (*C*) Flow in the hepatic artery of the liver remnant decreases during portal hyperflow in ALPPS. (*C1*) In patients, hepatic artery flow decreases in the left hepatic artery to the regenerating lobe from 116 ± 8 to 71 ± 70 mL/min (##$P = .014$, $n = 15$), reflecting the buffer response of the hepatic artery to portal hyperflow. In contrast, it increases in the right hepatic artery to the deportalized lobe from 227 ± 80 to 446 ± 190 mL/min (#$P = .001$, $n = 15$) to buffer the lack of portal blood flow. Data are given as single data points, depending on normality, as mean ± standard deviation or medians ± IQR. ANOVA (human data, $n = 15$) or Kruskal-Wallis test (rat data, $n = 4$) were performed for comparisons of groups.

fluorescence signal in a slide scanner and digital enlargement of positive signals at 3, 12, 24, and 72 hours (Fig 2, *C*). The proliferation rate of PVL and PVL + T was significantly higher compared with sham animals at 3, 24, and 72 hours, but interestingly not at 12 hours (Fig 2, *D*). Proliferation was significantly increased in PVL + T at 3, 24, and 72 hours when compared with PVL. There was no difference at 12 hours between the 2 groups. The histologic proliferation data confirmed the findings of volume increase by CT in the rapid and the slow regeneration model and shows that the degree of Ki-67 staining correlates well with volumetrically measured liver growth, except for the 12 hour time point.

Portal vein ligation induces portal hyperflow in the regenerating liver in both the rapid and slow regeneration models. Flow in the main portal vein in 15 human patients before and after PVL + T, the first step of the so-called "ALPPS" operation in humans as reported elsewhere,[6,12] was 704 ± 210 mL/min at baseline. Flow did not change immediately after ligation and transection or 7 days later (Fig 3, *A1*). Given that 70–80% of the portal vein flow outflow is occluded in PVL + T, no reduction in prehepatic hepato-petal

volume flow in the main portal vein is indirect proof of more flow per remnant liver volume (20–30%) perfused (ie, "portal hyperflow"). Similarly in rats, volume flow in the main portal vein did not change from a baseline of 15 mL/min (12–16 mL/min), neither after 75% portal vein ligation and thereby flow space removal in PVL (Fig 3, *A2*), nor after PVL + T (Fig 3, *A3*). Portal vein pressures in humans undergoing PVL + T increased significantly from 12 ± 5 mm Hg prior to the procedure to 18 ± 4 mm Hg after ligation and transection and stayed elevated for 7 days (Fig 3, *B1*). Similarly in rats, portal vein pressures in the main portal vein undergoing PVL (Fig 3, *B2*) and PVL + T (Fig 3, *B3*) increased significantly after the portal vein ligation step. However, the added transection in PVL + T did not increase the pressure further (Fig 3, *B3*). Pressure remained elevated at 3, 12, and 24 hours in both the PVL and PVL + T groups.

Reduced arterial flow in PVL + T in patients. We measured arterial flow in the human liver remnant before and after the first stage of the "ALPPS" operation in humans. Flow in the left hepatic artery decreased significantly from 116 ± 80 mL/min at baseline to 71 ± 70 mL/min after PVL + T, likely an adaptation to the portal hyperflow, known as the hepatic arterial buffer response[10,18] (Fig 3, *C1*). This decrease in arterial flow remained unchanged for up to 7 days. The flow in right hepatic artery to the deportalized lobe after PVL + T increased from a baseline of 227 ± 80 mL/min to 446 ± 190 mL/min (Fig 3, *C1*). This upregulation in flow also may be explained by the hepatic arterial buffer response and remains unchanged for up to 7 days after the operation.

Pimonidazole staining demonstrates local tissue hypoxia in rapid regeneration. To identify hypoxic areas in the regenerating liver, pimonidazole was used as a well-known marker for detection of hypoxic tissues.[19] Immunohistochemistry showed no specific signal in sham-operated animals (Fig 4, *A*). Upon hepatic artery ligation in rats (positive control), staining in the zone around the central vein was found (Fig 4, *B*). No specific signal was identified in regenerating hepatic tissue after PVL (Fig 4, *C*). However, there was intense staining after PVL + T (Fig 4, *D*). We used immunofluorescence-stained slides for quantification (Fig 4, *E*) based on an algorithm to assess the contrast between specific and nonspecific staining (online only Data supplement). In this algorithm, the variance in pixel intensity of liver tissue was assessed. Relative values were calculated by setting the mean variance of liver slices after sham surgery at 0%, while the mean variance of all liver slices after hepatic artery ligation was set at 100% (Fig 4, *E*). While there was no difference between PVL and sham-operated animals, PVL + T showed significant hypoxia, comparable to hepatic artery ligation, in the regenerating liver lobe at 3 and 12 hours (Fig 4, *F*). HIF-1α expression quantified by immunohistochemistry was higher in PVL + T when compared with PVL alone (Fig 4, *G*).

Rapid regeneration can be induced in the slow regeneration model by activation of hypoxic signaling pathways. Prolyl hydroxylase domain (PHD) 1–3 oxygen-sensing enzymes are natural gatekeepers of the adaptive response to hypoxia.[20] Under normoxia, PHD are constantly marking the continuously transcribed and translated HIF-1α subunits for degradation, while in hypoxia, the substrate for hydroxylation is missing. As a consequence, HIF-1α is upregulated and activates numerous hypoxic signaling pathways. With the hypothesis of pharmacologically changing slow to rapid liver regeneration, the PHD inhibitor DMOG was given to animals prior to PVL (slow regeneration). This intervention led to an enlargement of the RML volume from a baseline of 2.5 ± 0.5 mL to a final volume 6.6 ± 0.4 mL at 72 hours with increases of 60 ± 14% at 24 hours, 88 ± 11% at 48 hours, and 134 ± 21% at 72 hours (Fig 5, *A*). This degree of volume increase was not different at any time point from PVL + T, and was significantly higher than the volume increases observed after PVL. Intraperitoneal injection of DMOG in rats undergoing sham surgery as a control led to no change in starting volume. DMOG in PVL also led to an increase in the proportion of Ki-67 positive cells (Fig 5, *B*). The mitotic activity after PVL + DMOG was even higher than after PVL + T ($P = .023$; Fig 5, *C*). There was no significant difference in the proportion of Ki-67 positive cells between sham-operated animals and sham-operated animals receiving DMOG prior to the operation. While DMOG given systemically before sham operation seemed to have no significant overall proliferative impact on liver tissue, when DMOG was applied locally to the surface of liver tissue, geographic areas of hypertrophy were visible on the liver surface (Fig 5, *D*). Ki-67 staining showed 1-mm-deep areas of high proliferation (Fig 5, *E*) compared with areas from control animals that appeared macroscopically normal ($P < .001$; Fig 5, *F*).

Reversing hypoxia by increasing oxygen delivery to the regenerating liver blunts rapid liver regeneration. ITPP is an allosteric effector of hemoglobin and enhances the capacity of hemoglobin to

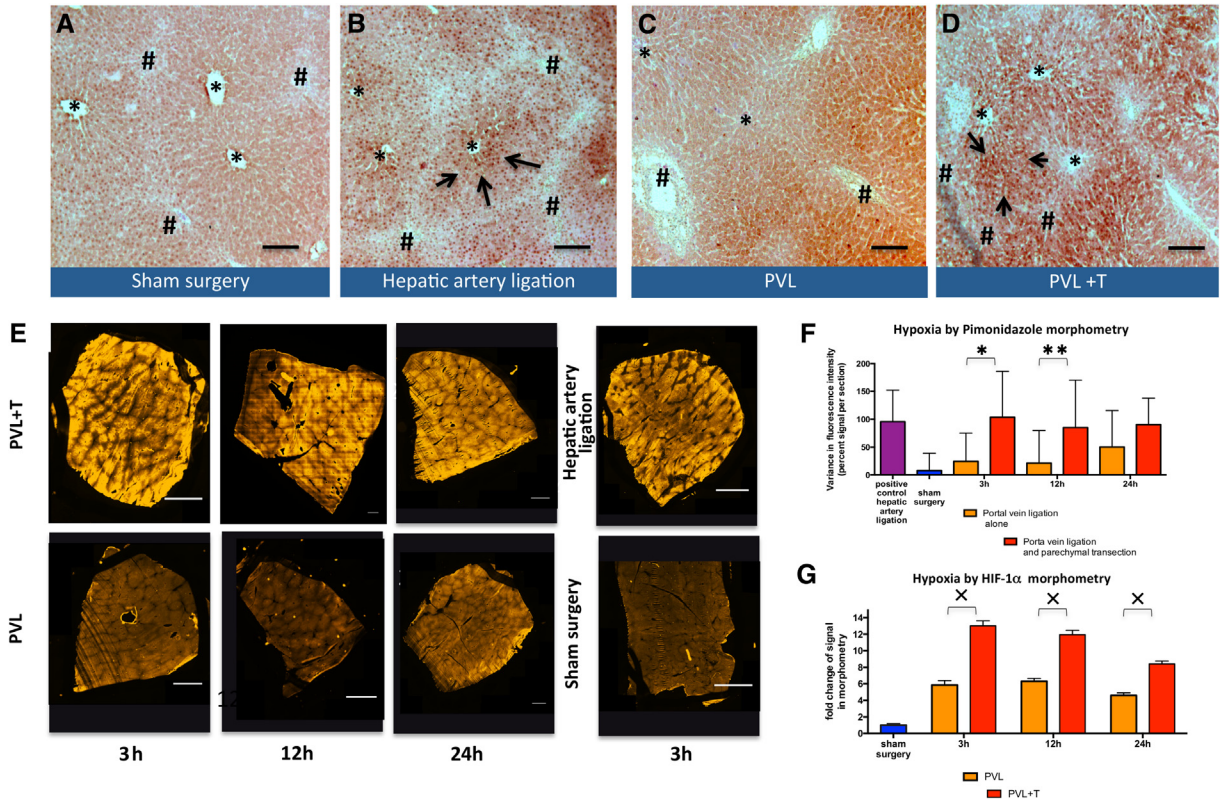

Fig 4. Hypoxia staining using pimonidazole in the regenerating liver lobe. (*A*) Pimonidazole immunohistochemistry shows no signal after sham surgery (negative control; *central veins, #portal tracts, scale bar: 100 mm). (*B*) After complete hepatic artery ligation, there is a strong signal around the central veins (*arrows*), a positive control for hypoxia (*central veins, #portal tracts, scale bars: 100 μm). (*C*) There is no specific pimonidazole staining of the liver tissue after portal vein ligation alone (PVL), while (*D*) PVL and transection (PVL + T) lead to distinct zone 2 hypoxia (*arrows*; *central veins, #portal tract). (*E*) The results obtained by immunohistochemistry were confirmed by immunofluorescence and quantified. Entire tissue blocks were exposed in an immunofluorescence slide scanner overnight to compare the variance of fluorescence intensity of regenerating liver tissue after PVL + T at 3, 12, and 24 hours and regenerating liver tissue after PVL and compared with sham surgery (3 h) and hepatic artery ligation (3 h; scale bars: 1,000 μm). (*F*) Hypoxia by pimonidazole morphometry. Variance of pimonidazol-positive versus pimonidazol-negative areas. Two-way ANOVA and multiple comparisons between groups ($n = 4$ animals per group with 4 sections per animal) were performed (*3 hours PVL 24 ± 51 vs PVL + T 104 ± 83, $P = .001$; **12 hours PVL 21 ± 59 vs PVL + T 85 ± 85, $P = .01$). At 24 hours, there was no significant difference. (*G*) Hypoxia by hypoxia-inducible factor-1α (HIF-1α) morphometry. HIF-1α positive cells were counted in 10 or 20 high-power fields in 4 animals per group and expressed in relation to sham-operated animals as x-fold change in signal. ANOVA and multiple comparisons were used to determine significance. There was a significant increase in HIF-1α signal in PVL + T at 3, 12, and 24 hours compared with PVL ($^{\times}P < .001$ for 3, 12, and 24 hours).

release oxygen in tissue.[21] It is well known that this compound substantially abrogates hypoxia in tumors, leading to reduced tumor growth.[22,23] We therefore tested to see if rapid regeneration could be abrogated by increasing oxygen delivery to the growing liver by treating the group of animals undergoing PVL + T. When given 12 hours before and at the first day after the operation, ITPP clearly reduced liver regeneration after PVL + T. Right median lobe volume changed from a baseline volume of 2.3 ± 0.2 mL to only 4.8 ± 0.6 mL at 72 hours ($P < .001$), a reduced volume increase over time (Fig 6, *A*). This volumetric growth was not different at any time point from growth after PVL, but significantly decreased compared with the volume increase observed after PVL + T. Intraperitoneal injection of ITPP in rats undergoing sham surgery led to no change in volumetry volume.

Application of ITPP prior to PVL + T led to less Ki-67 positive cells compared with PVL + T at 72 hours (Fig 6, *B*). The degree of mitotic activity in PVL + T plus ITPP was decreased significantly and not different from PVL (Fig 6, *C*). There was no significant difference in the proportion of

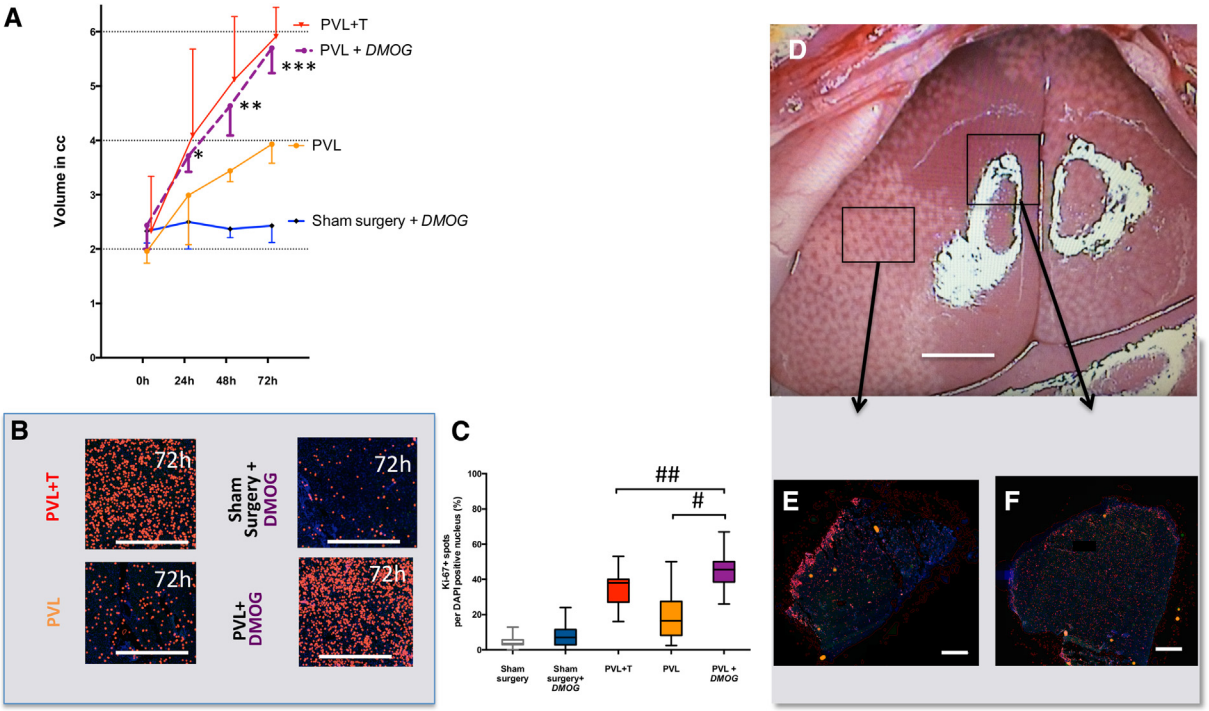

Fig 5. Pharmacologic activation of hypoxic-signaling pathways using prolyl-hydroxylase inhibitors. (*A*) Systemic application of dimethyloxaloglycine (DMOG) accelerates slow liver regeneration after portal vein ligation (PVL) to rapid liver regeneration for 72 hours. The differences in volume between PVL and PVL + DMOG are significant at *24 hours ($P = .028$), **48 hours ($P = .006$), and ***72 hours ($n = 8$; $P = .006$); data are mean ± standard deviations. ANOVA and multiple comparisons were used for comparison between groups. (*B*) Ki-67 staining of the right median lobe (RML) after 72 hours shows that DMOG added to PVL induces very high proliferative rates comparable in mitotic activity to portal vein ligation and transection (PVL + T). DMOG added to sham surgery alone does not increase proliferation. (*C*) Box plots (minimal to maximal value) show Ki-67 positive nuclei in percentage of DAPI-stained nuclei. Quantification was performed by evaluation of 20 high-power fields (HPFs) per animal. PVL + DMOG has 44 ± 10% signal compared with 19 ± 13% in the PVL group (#$P < .001$) and 35 ± 9% PVL + T (##$P = .023$). DMOG in animals undergoing sham surgery (8 ± 6%) results in no significant increase compared with sham surgery alone (4 ± 3%). ANOVA and multiple comparisons were used for comparison between groups. (*D*) Photograph of the geographic areas of liver regeneration visible on the surface of the entire liver after local application of DMOG onto the liver. (*E*) Representative Ki-67 staining of a mitotically active zone of 1-mm depth from the surface in areas of regeneration shows 40 ± 9% Ki-67 positive cells compared with (*F*) 3 ± 5% Ki-67 positive cells in areas of control liver tissue (scale bars in all photographs are 1,000 μm).

Ki-67 positive cells between sham-operated animals with or without ITTP treatment.

DISCUSSION

This study provides first evidence that hypoxia modulates the kinetic rate of liver regeneration. Our finding of hypoxia in liver remnants undergoing rapid liver regeneration was supported by the transformation of slow regeneration into rapid regeneration using a PHD inhibitor. In contrast, increase in oxygen delivery to the rapidly regenerating lobe using ITPP abrogated rapid regeneration and reduced it to the slow liver regeneration found after PVL. Importantly, the PHD inhibitor DMOG additionally triggered de-novo regeneration of 1 mm depth upon local application to rat livers without any portal vein manipulation. This group of drugs is currently in clinical phase III trials for applications unrelated to liver regeneration and will have to be evaluated as a therapeutic agent for drug-inducible liver regeneration. (see schematic Fig 7)

Based on our findings, hypoxia may be the rate determining mechanism for rapid regeneration after PVL + T. While there is no hypoxia present in the slowly regenerating liver after PVL, the regenerating lobe after PVL + T seems profoundly hypoxic as shown by pimonidazole staining. This degree of hypoxia may be explained by the reduction of oxygen-rich arterial flow in the regenerating liver lobe in PVL + T as assessed in our arterial flow studies in humans. In contrast, this mechanism may have little or no importance

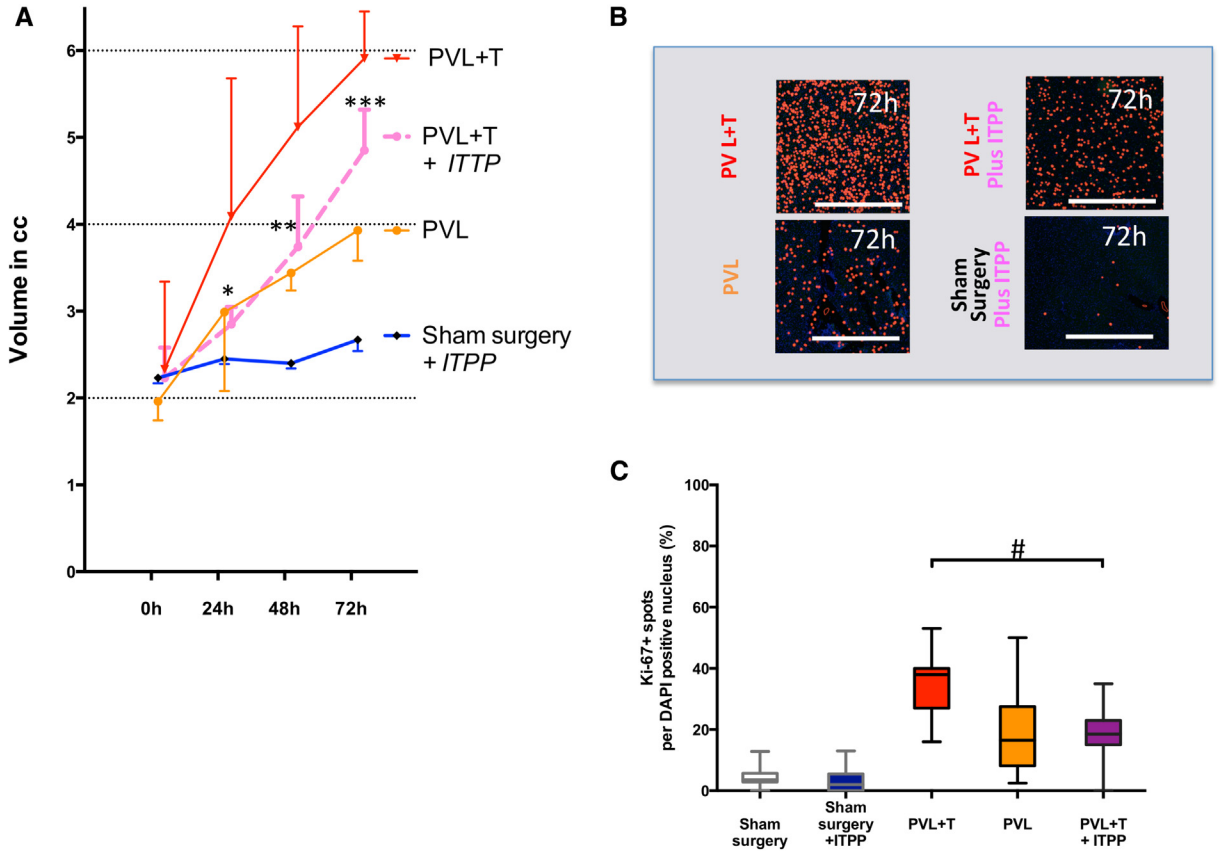

Fig 6. Pharmacologic deactivation of hypoxic signaling by increasing tissue oxygen delivery using myo-inositol-trispyrophosphate (ITPP). Systemic application of ITPP via an intraperitoneal injection decelerates rapid liver regeneration of portal vein ligation and transection (PVL + T) to slow liver regeneration. (*A*) Application of ITPP to rats undergoing PVL + T blunts rapid hypertrophy significantly to only a modest increase of 24 ± 6% at 24 hours (PVL + T: 74 ± 38%), 63 ± 18% at 48 hours (PVL + T: 111 ± 30%), and 107 ± 21% at 72 hours (PVL + T: 147 ± 16%). Volume increase after addition of ITPP is significantly lower compared with PVL + T at *24 hours ($P = .011$), **48 hours ($P = .006$), and ***72 hours ($n = 6$; $P = .003$). ANOVA and multiple comparisons were used for comparison between groups. (*B*) Ki-67 staining of the right median lobe (RML) 72 hours after PVL + T plus ITTP shows reduced mitotic activity after ITPP application, similar to PVL. Sham surgery and ITPP application alone serve as a negative control. (*C*) Box plots (minimal to maximal value) show Ki-67 positive nuclei in % of DAPI-stained nuclei. Quantification is performed by evaluation of 20 high-power fields per animal. PVL + T with additional ITPP had 18 ± 8% signal compared with 35 ± 9% in the PVL + T (#$P < .001$) and 19 ± 13% in PVL. PVL + T + ITPP show no difference compared to PVL ($P = .999$). ITPP in animals undergoing sham surgery results in no change compared with sham surgery alone. ANOVA and multiple comparisons were used for comparison between groups.

when there is compensatory blood flow between liver lobes through sinusoidal collaterals such as in PVL. Interestingly, reduced arterial flow has been demonstrated repeatedly in regenerating livers in animal models of partial hepatectomy,[24-26] small-for-size live donor liver transplantation[25,27] and in models of liver regeneration after PVL,[10] but its role as the accelerator of liver regeneration has so far not been understood.

In the rat model of PVL, we were not able to measure arterial flow to the regenerating lobe directly due to technical limitations, namely the unavailability of very small-volume flow probes. However, the precise physiological measurements by Rocheleau et al,[10] using radiolabeled microspheres, demonstrated that in the rat liver with portal hyperflow arterial flow is reduced from 1 mL/min to 0.5 mL/min. Interestingly, we also observed about 50% reduction in arterial flow in our human flow measurements. In the study by Rocheleau et al,[10] the liver with arterial flow grew in size. The authors also demonstrated a correlation between decreasing arterial flow in the regenerating lobe and increasing portal flow. Essential to keeping portal flow constant, hepatic arterial autoregulation was first described as the "hepatic

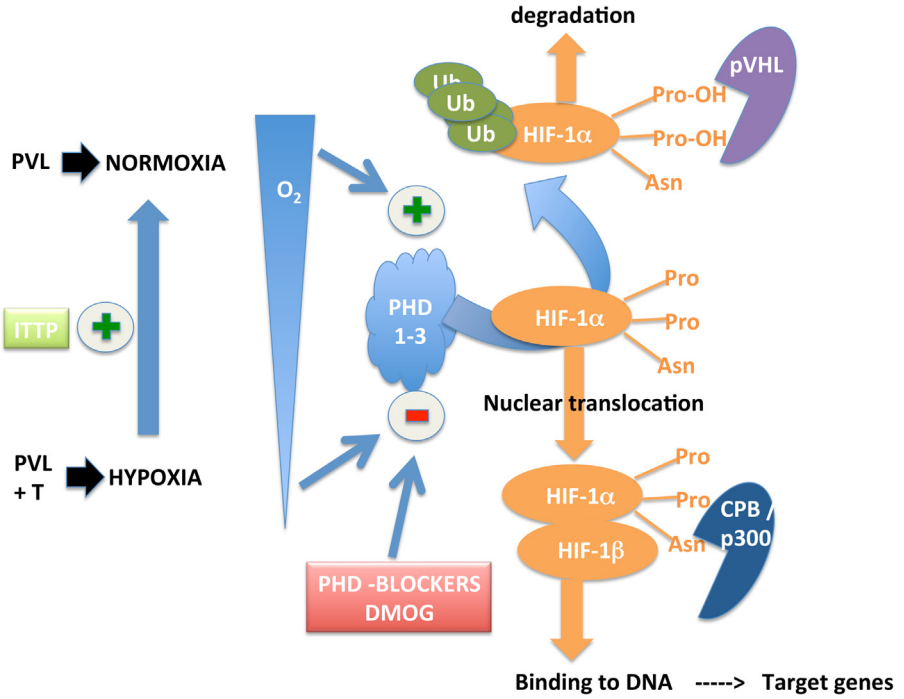

Fig 7. Schematic of the proposed mechanism of rapid hypertrophy induced by hypoxia of the liver remnant. Under normoxic conditions, like portal vein ligation (PVL), prolyl-hydroxylases 1-3 (PHD 1-3) hydroxylate prolyl residues on the HIF-1α, which leads to the binding of Von-Hippel-Landau protein (pVHL), ubiquinisation (Ub), and degradation of HIF-1α. Arterial hypoxia in portal vein ligation and transection (PVL + T) leads to a blockade of PHD 1-3, allowing binding of HIF-1α to the coactivators EA1 binding protein p300/CREB binding protein (P300/CBP) and transcriptional activation of over 200 HIF-1α target genes, some of which may have a role in accelerating liver regeneration. Dimethyloxalylglycine (DMOG) blocks PHD 1-3 and thereby allows HIF-1α stabilization in cells, induction of hypoxia signaling, and acceleration of liver regeneration. Myo-inositol tri-pyrophosphate (ITTP) increases oxygen delivery by allosteric conformational change of the hemoglobin molecule and thereby restores normoxia, blunting rapid liver regeneration.

arterial buffer response"[11] and was explained by the differential washout of adenosine with different degrees of portal flow.[18] Interestingly, based on this physiological effect, hypoxia has been postulated repeatedly to "accompany" liver regeneration.[5,10] In stark contrast to our findings, hypoxia has been viewed by most as detrimental to liver regeneration,[28] and abrogating hypoxia through surgical maneuvers, like portal vein arterialization, has been considered beneficial to the regenerating liver.[25]

Recently, investigators described the presence of the master regulator of hypoxia HIF-1α in regenerating livers after resection,[29,30] not just in response to hypoxic injury but as an important regulator of hepatic metabolism in general.[31,32] It also has been demonstrated that liver regeneration is actually increased in mice deficient for PHD-1 and that increased HIF-1α activity in the regenerating liver not only induced a protective response, but also accelerated liver regeneration.[33] We actually speculated that hypoxia sensing might be used therapeutically in extended liver resections and liver transplantation, and our study supports these ideas. Our finding of differential degrees of liver regeneration after portal vein manipulation and the pro-mitotic effect of the local application of a PHD inhibitor allowed us to show that hypoxia sensing not only enhances liver regeneration, but also may serve as an initiator of liver regeneration independently of portal hyperflow.

Very recently, the powerful effect of stabilization of HIF-1α, and thereby hypoxia sensing on regenerative processes, has been pointed out in a model of epidermal wound healing.[34] It was shown that the PHD inhibitor 1,4-dihydrophenonthrolin-4-one-3-carboxylic acid used in a local gel application in B6 mice in the ear punch hole model leads to accelerated wound healing via the dedifferentiation and mobilization of progenitor cells. We speculate that similar processes of cell reprogramming to glycolytic progenitor cells in the liver and further generation of hepatocytes from progenitor cells may be initiated and controlled by arterial flow

restriction in the regenerating liver, inducing hypoxia-signaling pathways. Which cells constitute these progenitor cells remains unclear. Using Ki-67 staining, we observed 2 peaks of proliferation: 1 immediately after the procedure at 3 hours, followed by a decrease in proliferative activity at 12 hours and then an increase at 24 hours. It is well known that 2 stages of liver regeneration occur.[35-37] The first consists of the activation of signaling pathways, including growth factors, cytokines, neuroendocrine factors, and paracrine signals (called priming phase), peaking between 2–3 hours after the operation. It is followed by a second proliferative phase with hepatocyte DNA synthesis,[37] with maximum activity between 24 and 48 hours. While in our study regeneration activity in the liver with PVL seems to be absent in the priming phase at 3 hours, there is proliferation in the PVL + T at this very early stage. PVL + T may accentuate the priming phase of regeneration. Additional study will help us learn why this early proliferation occurs. Hypoxia in PVL + T may induce early cell proliferation. Through transection, collateral flow between RML and LML is interrupted completely, which further increases the concentration of growth and inflammatory mediators in the RML, possibly accentuating and accelerating regeneration processes.

Several groups have presented animal models of the PVL + T procedure.[38,39] One study in rats demonstrated accelerated hypertrophy of the RML after PVL + T, the same model we used. The authors hypothesized that interruption of vascular shunts between the deportalized and the regenerating liver may explain rapid hypertrophy in PVL + T,[38] but they did not assess the hemodynamic effects of the operation. They speculated that the increased growth rate of PCL + T may be explained by hepatocellular damage and necrotic areas in the deportalized LML via an increased expression pattern of inflammatory mediators, like IL-6 and TNF-α. Another study examined PVL + T, but the authors did not really use a model of rapid hypertrophy without mass reduction. They combined liver resection of the left lateral lobe with PVL + T, and thereby created a partial liver resection and portal vein occlusion model at the same time. Their study suggested that rapid hypertrophy was purely a result of systemic trauma induced by the transection of the liver and also could be induced by operative damage to the spleen and lungs.[39] However, in our study, PVL combined with tourniquet instead of transection also induced an acceleration of volumetric growth similar to reports in patients undergoing PVL with tourniquet ligation instead of transection.[9] Therefore, our study supports the concept that abrogation of collateral flow, rather than the trauma caused by transection alone, plays the key role in modulating regenerative kinetics.

Flow and pressure measurements in patients undergoing PVL + T as a liver resection strategy revealed that flow volume in the main portal vein did not change after PVL + T. However, an increase in portal vein pressure was observed. These findings were confirmed in our rat model. Given these findings, we conclude that portal hyperflow, arithmetically 4 times the flow per tissue unit, results in increased portal vein pressures in PVL as well as PVL + T. We further investigated the hepatic arterial buffer response in the regenerating liver. Flow measurement in humans showed that the hepatic arterial flow to the regenerating liver was decreased significantly in PVL + T. The observation that transaminases are significantly higher after PVL + T than they are after PVL alone, in our experience and in both experimental articles on PVL + T,[38,39] may be explained by hypoxic cell death rather than by the trauma of transection.

Because we were unable to measure rat arterial volume flow, we chose to induce hypoxia sensing by activating HIF-1α pathway in the regenerating lobe after PVL using the well-established PHD inhibitor DMOG. We hypothesized that this might increase the regenerative rate in the same way that adding a transection between the lobes would. DMOG given to rats undergoing PVL induced a similar acceleration of regeneration as performing a transection between the regenerating and the deportalized lobe. Interestingly, we observed that the local application of DMOG to rat livers also induced a 1-mm deep area of liver regeneration of hepatic tissue without any portal vein manipulation. While augmentation of liver regeneration has been reported after partial hepatectomy in PHD-1 knockout mice,[33] a triggering role for regeneration without liver resection has so far not been described.

DMOG, however, may influence other pathways beyond HIF-1α subunit stabilization. To demonstrate that hypoxia sensing is the catalyst of rapid hypertrophy, we needed to confirm that increase of tissue oxygen abrogates rapid hypertrophy and switches the rapid to the slow regeneration. We therefore used ITPP as an allosteric hemoglobin regulator to increase oxygen delivery to liver tissue. Rapid hypertrophy with the high mitotic rate was blunted substantially.

In conclusion, this study includes patient and animal data to provide the first evidence that hemodynamic changes and resulting hypoxia may explain rapid liver regeneration. It also points out the possible potential of PHD inhibitors to accelerate the slow regeneration associated with portal vein occlusion. Pharmacologic simulation of hypoxia may offer clinical advantages and may replace the surgical practice of PVL + T in the form of "ALPPS," an operation that, while opening new surgical options, has been proven to be fraught with complications and a prohibitively high mortality rate.[40,41]

We acknowledge the contribution of Tobias Piegeler, MD to the collection of data for the animal experiment and to the drafting of the first version of this paper.

SUPPLEMENTARY DATA

Supplementary data related to this article can be found online at http://dx.doi.org/10.1016/j.surg.2016.05.018.

REFERENCES

1. Michalopoulos GK. Liver regeneration after partial hepatectomy: Critical analysis of mechanistic dilemmas. Am J Pathol 2010;176:2-13.
2. Kinoshita H, Sakai K, Hirohashi K, Igawa S, Yamasaki O, Kubo S. Preoperative portal vein embolization for hepatocellular carcinoma. World J Surg 1986;10:803-8.
3. van Lienden KP, van den Esschert JW, de Graaf W, Bipat S, Lameris JS, van Gulik TM, et al. Portal vein embolization before liver resection: A systematic review. Cardiovasc Intervent Radiol 2013;36:25-34.
4. Nadalin S, Testa G, Malago M, Beste M, Frilling A, Schroeder T, et al. Volumetric and functional recovery of the liver after right hepatectomy for living donation. Liver Transpl 2004;10:1024-9.
5. Abshagen K, Eipel C, Vollmar B. A critical appraisal of the hemodynamic signal driving liver regeneration. Langenbecks Arch Surg 2012;397:579-90.
6. Schnitzbauer AA, Lang SA, Goessmann H, Nadalin S, Baumgart J, Farkas SA, et al. Right portal vein ligation combined with in situ splitting induces rapid left lateral liver lobe hypertrophy enabling 2-staged extended right hepatic resection in small-for-size settings. Ann Surg 2012;255:405-14.
7. Schadde E, Schnitzbauer AA, Tschuor C, Raptis DA, Bechstein WO, Clavien PA. Systematic review and meta-analysis of feasibility, safety, and efficacy of a novel procedure: Associating liver partition and portal vein ligation for staged hepatectomy. Ann Surg Oncol 2015;22:3109-20.
8. Schadde E, Malago M, Hernandez-Alejandro R, Li J, Abdalla E, Ardiles V, et al. Monosegment ALPPS hepatectomy: Extending resectability by rapid hypertrophy. Surgery 2015;157:676-89.
9. Robles R, Parrilla P, Lopez-Conesa A, Brusadin R, de la Pena J, Fuster M, et al. Tourniquet modification of the associating liver partition and portal ligation for staged hepatectomy procedure. Br J Surg 2014;101:1129-34; discussion 34.
10. Rocheleau B, Ethier C, Houle R, Huet PM, Bilodeau M. Hepatic artery buffer response following left portal vein ligation: Its role in liver tissue homeostasis. Am J Physiol 1999;277:G1000-7.
11. Lautt WW, Legare DJ, d'Almeida MS. Adenosine as putative regulator of hepatic arterial flow (the buffer response). Am J Physiol 1985;248:H331-8.
12. Schadde E, Ardiles V, Slankamenac K, Tschuor C, Sergeant G, Amacker N, et al. ALPPS offers a better chance of complete resection in patients with primarily unresectable liver tumors compared with conventional-staged hepatectomies: Results of a multicenter analysis. World J Surg 2014;38:1510-9.
13. Sears JE, Hoppe G, Ebrahem Q, Anand-Apte B. Prolyl hydroxylase inhibition during hyperoxia prevents oxygen-induced retinopathy. Proc Natl Acad Sci U S A 2008;105:19898-903.
14. Biolo A, Greferath R, Siwik DA, Qin F, Valsky E, Fylaktakidou KC, et al. Enhanced exercise capacity in mice with severe heart failure treated with an allosteric effector of hemoglobin, myo-inositol trispyrophosphate. Proc Natl Acad Sci U S A 2009;106:1926-9.
15. Yeh KY, Yeh M, Polk P, Glass J. Hypoxia-inducible factor-2alpha and iron absorptive gene expression in Belgrade rat intestine. Am J Physiol Gastrointest Liver Physiol 2011;301:G82-90.
16. Team RC. R: A language and environment for statistical computing. Vienna: Austria; 2014. Available from: https://www.r-project.org/.
17. Pau G, Fuchs F, Sklyar O, Boutros M, Huber W. EBImage—An R package for image processing with applications to cellular phenotypes. Bioinformatics 2010;26:979-81.
18. Lautt WW, Legare DJ, Ezzat WR. Quantitation of the hepatic arterial buffer response to graded changes in portal blood flow. Gastroenterology 1990;98:1024-8.
19. Terada N, Ohno N, Saitoh S, Ohno S. Immunohistochemical detection of hypoxia in mouse liver tissues treated with pimonidazole using "in vivo cryotechnique". Histochem Cell Biol 2007;128:253-61.
20. Appelhoff RJ, Tian YM, Raval RR, Turley H, Harris AL, Pugh CW, et al. Differential function of the prolyl hydroxylases PHD1, PHD2, and PHD3 in the regulation of hypoxia-inducible factor. J Biol Chem 2004;279:38458-65.
21. Teisseire B, Ropars C, Villereal MC, Nicolau C. Long-term physiological effects of enhanced O2 release by inositol hexaphosphate-loaded erythrocytes. Proc Natl Acad Sci U S A 1987;84:6894-8.
22. Derbal-Wolfrom L, Pencreach E, Saandi T, Aprahamian M, Martin E, Greferath R, et al. Increasing the oxygen load by treatment with myo-inositol trispyrophosphate reduces growth of colon cancer and modulates the intestine homeobox gene Cdx2. Oncogene 2013;32:4313-8.
23. Raykov Z, Grekova SP, Bour G, Lehn JM, Giese NA, Nicolau C, et al. Myo-inositol trispyrophosphate-mediated hypoxia reversion controls pancreatic cancer in rodents and enhances gemcitabine efficacy. Int J Cancer 2014;134:2572-82.
24. Eipel C, Abshagen K, Vollmar B. Regulation of hepatic blood flow: The hepatic arterial buffer response revisited. World J Gastroenterol 2010;16:6046-57.
25. Eipel C, Abshagen K, Ritter J, Cantre D, Menger MD, Vollmar B. Splenectomy improves survival by increasing arterial blood supply in a rat model of reduced-size liver. Transpl Int 2010;23:998-1007.
26. Blumgart LH. Liver atrophy, hypertrophy and regenerative hyperplasia in the rat: The relevance of blood flow. Ciba Found Symp 1977:181-205.

27. Smyrniotis V, Kostopanagiotou G, Kondi A, Gamaletsos E, Theodoraki K, Kehagias D, et al. Hemodynamic interaction between portal vein and hepatic artery flow in small-for-size split liver transplantation. Transpl Int 2002;15:355-60.
28. Mortensen KE, Revhaug A. Liver regeneration in surgical animal models—A historical perspective and clinical implications. Eur Surg Res 2011;46:1-18.
29. Maeno H, Ono T, Dhar DK, Sato T, Yamanoi A, Nagasue N. Expression of hypoxia inducible factor-1alpha during liver regeneration induced by partial hepatectomy in rats. Liver Int 2005;25:1002-9.
30. Schmeding M, Rademacher S, Boas-Knoop S, Roecken C, Lendeckel U, Neuhaus P, et al. rHuEPo reduces ischemia-reperfusion injury and improves survival after transplantation of fatty livers in rats. Transplantation 2010;89:161-8.
31. Tajima T, Goda N, Fujiki N, Hishiki T, Nishiyama Y, Senoo-Matsuda N, et al. HIF-1alpha is necessary to support gluconeogenesis during liver regeneration. Biochem Biophys Res Commun 2009;387:789-94.
32. Yoon D, Okhotin DV, Kim B, Okhotina Y, Okhotin DJ, Miasnikova GY, et al. Increased size of solid organs in patients with Chuvash polycythemia and in mice with altered expression of HIF-1alpha and HIF-2alpha. J Mol Med (Berl) 2010;88:523-30.
33. Mollenhauer M, Kiss J, Dudda J, Kirchberg J, Rahbari N, Radhakrishnan P, et al. Deficiency of the oxygen sensor PHD1 augments liver regeneration after partial hepatectomy. Langenbecks Arch Surg 2012;397:1313-22.
34. Zhang Y, Strehin I, Bedelbaeva K, Gourevitch D, Clark L, Leferovich J, et al. Drug-induced regeneration in adult mice. Sci Transl Med 2015;7:290ra92.
35. Fausto N, Mead JE. Regulation of liver growth: Protooncogenes and transforming growth factors. Lab Invest 1989;60:4-13.
36. Taub R. Liver regeneration 4: Transcriptional control of liver regeneration. FASEB J 1996;10:413-27.
37. Michalopoulos GK. Liver regeneration. J Cell Physiol 2007;213:286-300.
38. Yao L, Li C, Ge X, Wang H, Xu K, Zhang A, et al. Establishment of a rat model of portal vein ligation combined with in situ splitting. PLoS One 2014;9:e105511.
39. Schlegel A, Lesurtel M, Melloul E, Limani P, Tschuor C, Graf R, et al. ALPPS: From human to mice highlighting accelerated and novel mechanisms of liver regeneration. Ann Surg 2014;260:839-46; discussion 46-7.
40. Dokmak S, Belghiti J. Which limits to the "ALPPS" approach? Ann Surg 2012;256:e6; author reply e16-7.
41. Schadde E, Ardiles V, Robles-Campos R, Malago M, Machado M, Hernandez-Alejandro R, et al. Early survival and safety of ALPPS: First report of the International ALPPS Registry. Ann Surg 2014;260:829-36; discussion 36-8.

Supporting information

Hypoxia Triggers Rapid Liver Regeneration: a Translational Approach from Patients Back to an Animal Model

Erik Schadde,[1,2,3] Christopher Tsatsaris,[1] Stefan Breitenstein,[3] Martin Urner,[1,4] Tobias Piegeler,[4] Roman Schimmer,[1] Christa Booy,[1] Birgit Roth Z'graggen,[1] Roland H. Wenger,[1] Donat R. Spahn,[4] Martin Hertl,[2] Martin Schläpfer,[1,4] Beatrice Beck-Schimmer[1, 4, 5]

Installation of Bioconductor and EBImage library

To run the following code, please install the latest release of R (https://www.r-project.org/), then get the latest version of Bioconductor by starting R and entering the commands:

```
source("http://bioconductor.org/biocLite.R")
biocLite("EBImage")

# Load EbImage library
library("EBImage")
```

Generation of a fusion image based on DAPI- and Ki-67-stained liver slices

This function highlights matching Ki-67 and DAPI fluorescence spots after fusion of images "ki67_img" and "dapi_img". A highlighted RGB Image is written to disk to allow a later visual verification of the automated quantification procedure.

```
Computeki67Image <- function(ki67_img, dapi_img)
{
    # Read images
    ximg1 <- readImage(ki67_img)
    ximg2 <- readImage(dapi_img)

    # Convert to gray scale
    b <- channel(ximg2, "gray") # DAPI
    r <- channel(ximg1, "gray") # ki67

    # Track down spots in k67 stainings
    # by thresholding intensities between 80-100%
    ximg1_flat <- ximg1 > 0.8
    ximg1_flat[ximg1_flat >  0.8] <- 1

    # Apply bitwise AND to merge DAPI and ki67 stainings
    z_img <- b & channel(ximg1_flat, "gray")

    # Dilate matched spots
    kern = makeBrush(7, shape='disc')
    z_img2 = dilate(z_img, kern)
```

```
    # Estimate area of the liver slice in both stainings
    # First, the DAPI staining
    negmask1 <- b
    negmask1[negmask1 > 0.1] <- 1
    negmask1[negmask1 < 1] <- 0

    # Second, the ki67 staining
    negmask2 <- r
    negmask2[negmask2 > 0.1] <- 1
    negmask2[negmask2 < 1] <- 0

    # Combine the mask using bitwise AND
    negmask <- negmask1 | negmask2

    # Filter out black holes in the slice area
    negmask = gblur(negmask, sigma=6)
    negmask[negmask > 0.01] <- 1
    negmask[negmask < 1] <- 0

    # Do segmentation procedure
    c <- bwlabel(negmask)

    # Compose a merged rgbImage
    fximg <- rgbImage(green=channel(ximg1, "gray"),
                blue=channel(ximg2, "gray"),
                red=z_img2)

   # Compose a merged rgbImage and write it to disk
    res = paintObjects(c, fximg, col='#ff0000', thick=TRUE)
    writeImage(res, paste(ki67_img, "_marked.png"), 'png')

    # Return the data in data.frame
    return filename=ki67_img
}
```

Determination of mean fluorescence intensity in pimonidazole-stained liver slices

This function calculates the mean pixel intensity of the largest, contiguous area of a tissue slice contained “fname”. A highlighted RGB Image is written to disk to allow a later visual verification of the automated quantification procedure.

```
ComputePimonidazoleImage <- function(fname)
  {
    # Read image file
    ximg = readImage(fname)

    # Threshold pixel intensities above 10%
    ximg2 <- ximg > 0.1

    # Deal with black spots in the respective area
    g_t = fillHull(ximg2)

    # Basic morphological operations facilitating the segmentation
    kern = makeBrush(10, shape='disc')
    g_t2 = dilate(erode(g_t, kern), kern)
    kern3 = makeBrush(50, shape='disc')
    g_t3 = erode(g_t2, kern3)

    # Do the segmentation procedure
    cmask = bwlabel(g_t3)
    b = channel(cmask,"r")

    # Write an RGB image for visual verification
    res = paintObjects(b, ximg, col='#ff0000', thick=TRUE)
    writeImage(res, paste(fname, '_marked.tiff'), 'tiff')

    # Compute mean pixel intensity of the largest, contiguous area
    ft = computeFeatures(b, res)
    xy <- which.max(ft[, "x.0.s.area"])
    imean <- ft[ xy , "x.a.b.mean"]
    isd <- ft[ xy , "x.a.b.sd"]
   # Return the data in a data.frame
    z <- data.frame(fname=fname, m=imean, s=isd)
    return(z)
}
```